31 p.

[redacted]

[redacted]

NASA TECHNICAL MEMORANDUM

NASA

NASA TM X-52040

NASA TM X-52040

[redacted]

PROPELLANT HEATING STUDIES WITH WALL AND NUCLEAR HEATING

by B. H. Anderson, S. C. Huntley, and D. J. Connolley
Lewis Research Center
Cleveland, Ohio

TECHNICAL PREPRINT prepared for Winter Annual Meeting of the American Society of Mechanical Engineers New York, New York, November 29-December 4, 1964

NATIONAL AERONAUTICS AND SPACE ADMINISTRATION · WASHINGTON, D.C. · 1964

[redacted]

TECHNICAL MEMORANDUM

PROPELLANT HEATING STUDIES WITH WALL AND NUCLEAR HEATING

by B. H. Anderson, S. C. Huntley, and D. J. Connolley
Lewis Research Center
Cleveland, Ohio

TECHNICAL PREPRINT prepared for

Winter Annual Meeting
of the American Society of Mechanical Engineers
New York, New York, November 29-December 4, 1964

NATIONAL AERONAUTICS AND SPACE ADMINISTRATION

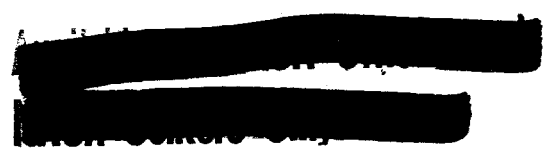

PROPELLANT HEATING STUDIES WITH WALL AND NUCLEAR HEATING

by B. H. Anderson, S. C. Huntley, and D. J. Connolley

Lewis Research Center

E-2682

INTRODUCTION

One problem in the design of nuclear space vehicles is the inability to determine the effects that heating of the propellant have on the weight optimization of the vehicle system. For a given set of heating conditions a knowledge of the state of the liquid is fundamental to meet the pump requirements. For a given set of pump requirements, the appropriate liquid state can be achieved in two ways: (1) use thermal insulation and nuclear shielding to prevent excessive temperature rise, or (2) increase the tank pressure to compensate for the propellant temperature rise. Both of these methods, however, necessitate an increase in the gross weight of the vehicle. It is apparent that employment of either method to optimize the vehicle weight requires a knowledge of the state of the liquid.

The state of the liquid can be critically dependent on the heat-transfer processes involved. The vehicle will receive thermal radiation from three sources, direct solar radiation, planetary radiation, and albedo or reflected radiation. This type of heating gives rise to natural convection boundary layer flow along the tank wall. The warm fluid carried by the boundary layer accumulates at the liquid surface to form a stratified layer. For a nuclear vehicle, the propellant will also receive radiation in the form of gamma rays and neutrons that leak cut of the reactor and by capture gamma rays that are born when thermal

neutrons are absorbed. Nuclear radiation has the effect of increasing the kinetic energy of the propellant molecule. This increase in the kinetic energy of the molecule is felt locally in the form of heat. Thus nuclear radiation can be characterized as source heating, which is non-uniform in nature because of the absorption properties of the propellant. This type of heating is inherently unstable and gives rise to turbulent mixing. Relatively little information is available on the flow and heat transfer of a confined fluid subjected to the types of heating described, in particular when the fluid is contained by practical types of tank geometries.

Most of the work on the problem of analyzing the state of the liquid has been of a semi-empirical nature with little or no experimental verification. In reference 1, equations are presented that give the dimensionless parameters involved in the establishment of temperature gradients in a nondraining cylindrical tank. An approximate treatment of the propellant heating problem appears in references 2 and 3. In reference 2 an analytical flow model was developed that is primarily concerned with the development of the stratified layer in the course of time for the nondraining tank. Reference 3 presents an approximate numerical approach to the stratified layer problem for both draining and nondraining tanks. A simplified flow model is postulated where the temperature profile in the stratified layer is considered to develop in a series of finite sublayers; the temperature is constant within each layer but variable between layers.

In an effort to obtain further information on the flow behavior induced by wall and nuclear heating, an investigation was initiated at the

NASA-Lewis Research Center concurrent with the work of references 1, 2, and 3 and is presented herein. This investigation was conducted in three phases. In the first phase, the important factors relating to the basic flow behavior of a confined fluid subjected to wall and simulated nuclear heating were studied in a small-scale 1-gallon-capacity tank. Nuclear heating was simulated by permitting infrared radiation to be absorbed in a solution of two parts trichloroethane to one part ethyl alcohol. This first phase of the investigation, published in reference 4, provided visual studies of flow behavior and experimental information upon which a theoretical flow model was based. The second phase consisted of an analytical study using this flow model to predict the liquid temperature gradient as a function of time after the start of flow when a tank is subjected to wall and/or nuclear heating. In the third phase, a series of liquid hydrogen experiments were performed to investigate the behavior of liquid hydrogen subjected to (1) wall heating and (2) wall and source heating in a nuclear radiation field. These experiments were carried out in 125-gallon liquid hydrogen tanks. The analysis developed in the second phase was applied to predict the results of the hydrogen experiments.

SYMBOLS

$A(x)$ cross-sectional area of tank

$a(x_s)$ parameter defined by eq. (12)

$b(x_s)$ parameter defined by eq. (13)

C_p specific heat

$F(x_s)$ parameter defined by eq. (18)

$f(x_s)$ parameter defined by eq. (14)

$G(x_s)$	parameter defined by eq. (19)
L	initial liquid level
n	parameter defined by eq. (10)
$Q(x_s)$	parameter defined by eq. (22)
$Q_w(x_s)$	parameter defined by eq. (8)
$Q_n(x_s)$	parameter defined by eq. (8)
q_w	wall heating flux
q_n	nuclear heat deposition
T	temperature
t	time
$\dot{W}_p$	mass flow rate
x	axial distance measured from tank bottom
$\alpha(x_s)$	parameter defined by eq. (20)
$\beta(x_s)$	parameter defined by eq. (21)
δ	thickness of stratified layer
$\Phi(x,x_s)$	parameter defined by eq. (16)
$\varphi(x,x_s)$	parameter defined by eq. (5)
$\Psi(x,x_s)$	parameter defined by eq. (17)
$\psi(x,x_s)$	parameter defined by eq. (5)
ρ	density
σ	surface area
ϑ	temperature difference, $T - T_i$

Subscripts:

i	initial conditions
n	nuclear heating contribution

ref reference conditions

s surface conditions

s,ℓ limiting conditions

w wall heating contribution

INFRARED EXPERIMENT

This experiment was designed primarily for direct visual observation of the fluid behavior induced by simulated nuclear heating, wall heating, and a combination of the two types of heating. A simple apparatus was designed that permitted direct visual observation of the induced fluid motion. Nuclear heating was simulated by permitting infrared radiation to be absorbed in a solution of trichloroethane and ethyl alcohol.

Infrared rays are a form of electromagnetic radiation, which when absorbed by a fluid cause molecular agitation. This increase in the kinetic energy of the molecule is felt locally in the form of heat. The spectral absorption and hence the attenuation profile can be controlled to some extent by mixing fluids with different absorption characteristics. For this experiment, the solution mixture of two parts trichloroethane to one part ethyl alcohol gave a centerline heating profile that was similar to typical nuclear profiles.

Inasmuch as this work has been presented in detail in reference 4, only pertinent details are reviewed herein.

Experimental Apparatus

Figure 1 is a schematic diagram of the experimental arrangement consisting of a two-dimensional glass tank, infrared heating lamps, and support structure. The sides and bottom of the tank were fabricated

from 1/8-inch-thick pyrex plate glass and the front plates of the tank, through which the fluid motion was viewed, consisted of 1/4-inch-thick pyrex plate glass. The view tank was 12 inches high, 8 inches wide, and 2 inches deep (inside dimensions). The bottom portion of the tank had 4.26-inch-long sides that were set at angles of 45 degrees with respect to the tank axis. An outlet port was located in the bottom of the tank to permit the fluid to discharge. Access ports were located in the top of the tank for the fill line, vent line, and instrumentation. Three 1000-watt infrared lamps, located as shown in figure 1, provided variable heat input to the fluid. Each lamp was provided with a parabolic reflector to insure monodirectional radiation. The two vertical side walls of the tank were blackened to provide only wall heating. The slant and bottom sections were clear to allow the infrared radiation to penetrate the tank and be absorbed by the fluid.

Qualitative data of the induced fluid motion in the tank were obtained by use of a Schlieren system. In addition, axial temperature distributions were obtained with shielded thermocouples (see fig. 1).

Results and Discussion

Figure 2 shows axial temperature profiles at several times after start of heating with nonuniform source and wall heating for a nonflowing system. The results indicate that two distinct regions developed in the main bulk of fluid: an upper region where the effects of wall heating predominated to form a characteristic stratified layer, and a lower region where source heating dominated to form a uniform temperature profile. The two regions mentioned can also be seen in the Schlieren photograph presented in figure 3. Nonuniform source heating produced turbulent mixing with the

general motion tending to be upward. The fluid continued to rise until it encountered the stratified layer, which is a region of higher temperature. Upon encountering the stratified layer the buoyant force became zero, preventing the motion of fluid caused by source heating to penetrate the stratified layer.

Figure 4 presents the axial temperature profiles that were measured in the fluid at various times after start of heating for a flowing system with nonuniform source heating and wall heating. The results are essentially the same as for the nonflowing case except that the stratified layer is seen to be carried with the fluid during discharge.

ANALYSIS

The problem to be considered here is that of determining the temperature distribution within the propellant that results from nuclear and wall heating for a constant pressure discharge. The mathematical difficulties in solving the exact equations of motion for this problem are considerable. It was therefore thought desirable to obtain a solution by approximate methods. The method used herein abandons the attempt to satisfy the governing equations for every fluid particle, but chooses instead a plausible temperature profile in the tank that is made to satisfy the momentum and energy equation based on the entire fluid in the tank.

The first objective of the task was to develop a flow model on which an analysis could be based. This was accomplished by using the results obtained in the infrared experiments. The analysis that follows presents a summary of an analysis reported in an unpublished memorandum by B. H. Anderson, NASA Lewis Research Center.

Formulation of Analytical Flow Model

The heat that is distributed within the propellant is considered to have its origin from two sources, heat transfer from the walls of the tank and heating induced by the absorption of nuclear radiation. The criteria set down by Eckert (ref. 5), for determining whether forced or free convection is the dominant mechanism of heat transfer from the walls, indicate that a turbulent free convection boundary layer will form for most mission applications that have been considered. The free convection boundary layer thus established will carry warm fluid, as indicated in the infrared studies, toward the liquid surface to form a temperature gradient (see fig. 5). The temperature rise thus formed in this stratified layer as a result of wall heating is assumed to be of the form

$$T(x,t) - T_i = (T_s - T_i)\left(\frac{x - x_0}{\delta}\right)^n \qquad (1)$$

where $T(x,t)$ is the temperature within the stratified layer at station x at time t, $T_s - T_i$ is the difference between the surface and initial temperature, x_0 is the lower extremity of the stratified layer, δ is the thickness of the stratified layer, and n is an unknown factor to be determined.

That part of the heat induced by the absorption of nuclear radiation below the stratified layer is considered to form a uniform temperature profile. The temperature rise in this region is considered to have the form

$$T(t) - T_i = (T_s - T_i)f(t) \qquad (2a)$$

where the unknown function $f(t)$ represents the rise in the bulk temperature ratioed to the temperature difference $T_s - T_i$. The contribution of

the nuclear heating in the stratified layer is considered to be distributed according to the relation

$$T(x,t) - T_i = (T_s - T_i)f(t)\left[1.0 - \left(\frac{x - x_0}{\delta}\right)^n\right] \qquad (2b)$$

The distribution of wall and nuclear heating thus formulated by equations (1) and (2) is illustrated schematically in figure 5 by the temperature rise attributed to each contribution. At the liquid surface the temperature becomes $T(x_s,t) = T_s$, while the temperature rise contributed by the nuclear heating vanishes. At the lower extremity of the stratified layer, $x = x_0$, the wall contribution to temperature rise vanishes while temperature rise contributed by nuclear heating becomes $(T_s - T_i)f(t)$. The temperature profile within the stratified layer is obtained by adding that contributed from nuclear heating to the assumed wall temperature profile.

Growth of Stratified Layer

To obtain the development of the stratified layer in the course of time, it is assumed that the resulting temperature distribution in the fluid varies only in the axial direction. Thus, after introducing the liquid level x_s as the independent variable by means of the expression

$$\frac{d}{dt} = -\frac{\dot{W}_p}{\rho A(x_s)} \frac{d}{dx_s}$$

and assuming that the physical properties of the fluid do not vary significantly over the temperature range under consideration, the energy equation can be written in the form

$$\frac{d}{dx_s}\int_0^{x_s} \vartheta(x,x_s)A(x)dx - \vartheta(0,x_s)A(x_s) = -\frac{A(x_s)}{\rho\dot{W}_p}$$

$$\left[\int_0^{\sigma_s} q_w\, d\sigma + \int_0^{x_s} q_n(x)A(x)dx\right] \qquad (3)$$

As previously indicated, the temperature distribution in the propellant when nuclear and wall heating are present results in two distinct regions forming a lower region where the temperature is uniform and a stratified layer. From equations (1) and (2), the composite temperature profile can be written as

$$\vartheta(x,x_s) = \vartheta_{ref}\left[f(x_s)\varphi(x,x_s) + \psi(x,x_s)\right] \qquad (4)$$

where

$$\vartheta(x,x_s) = T(x,x_s) - T_i$$

$$\vartheta_{ref} = T_s - T_i$$

Consistent with the formulation of the flow model, the functions $\varphi(x,x_s)$ and $\psi(x,x_s)$ can be written explicitly as

$$\begin{aligned}
\psi(x,x_s) &= \left(\frac{x - x_0}{\delta}\right)^n && x_0 \le x \le x_s \\
\psi(x,x_s) &= 0 && 0 \le x < x_0 \\
\varphi(x,x_s) &= 1.0 - \left(\frac{x - x_0}{\delta}\right)^n && x_0 \le x \le x_s \\
\varphi(x,x_s) &= 1.0 && 0 \le x < x_0
\end{aligned} \qquad (5)$$

Introducing equation (4) into equation (3) and making the assumption that the contribution of wall and nuclear heating can be uncoupled in the energy equation, then equation (3) can be written as

$$\frac{d}{dx_s}\int_{x_0}^{x_s}\psi(x,x_s)A(x)dx = -Q_w(x_s) \tag{6}$$

$$\frac{d}{dx_s}\int_{0}^{x_s} f(x_s)\varphi(x,x_s)A(x)dx - f(x_s)A(x_s) = -Q_n(x_s) \tag{7}$$

where

$$Q_w(x_s) = \frac{A(x_s)}{C_p\dot{W}_p\vartheta_{ref}}\int_0^{\sigma_s} q_w\, d\sigma$$

$$Q_n(x_s) = \frac{A(x_s)}{C_p\dot{W}_p\vartheta_{ref}}\int_0^{x_s} q_n(x)A(x)dx \tag{8}$$

The left hand side of equation (6) can be integrated by successive integration by parts, thus

$$\frac{d}{dx_s}\left[\frac{\delta(x_s)A(x_s)}{(n+1)} - \frac{\delta^2(x_s)\frac{d}{dx_s}A(x_s)}{(n+1)(n+2)} + \frac{\delta^3(x_s)\frac{d^2}{dx_s^2}A(x_s)}{(n+1)(n+2)(n+3)} - \cdots\right] = -Q_w(x_s) \tag{9}$$

The a posteriori assumption is now made that the exponent n is not a function of time. By considering a cylindrical geometry, the solution for n can be obtained from equation (9) and the momentum equation written for the cylindrical tank. This gives

$$n = 3.94\,\frac{\vartheta_{ref}}{\vartheta_w} - 1.0 \tag{10}$$

The assumption is now made that equation (10) is a valid first order approximation for the exponent n, which may be used for noncylindrical

geometries. The stratified layer growth can now be evaluated from equation (9) for the general tank geometry.

The lower extremity of the stratified layer is given by the relation

$$x_0 = x_s - \delta(x_s) \tag{11}$$

The period of growth of the stratified layer can now be explicitly defined as $0 \leq x_0 \leq x_s$. Defining the location of the liquid level when $x_0 = 0$ as $x_{s,l}$, then a later period is defined as $0 \leq x_s \leq x_{s,l}$, in which the exit port feels the presence of the stratified layer.

Temperature Distribution in Initial Period

The solution of the temperature profile in the propellant during the growth of the stratified layer can now be obtained from equation (7). Thus, after simplification, equation (7) becomes

$$\frac{df}{dx_s}\int_0^{x_s} \varphi(x,x_s)A(x)dx + f(x_s)\frac{d}{dx_s}\int_{x_0}^{x_s} \psi(x,x_s)A(x)dx = -Q_n(x_s)$$

setting

$$a(x_s) = \int_0^{x_s} \varphi(x,x_s)A(x)dx \tag{12}$$

$$b(x_s) = \frac{d}{dx_s}\int_{x_0}^{x_s} \psi(x,x_s)A(x)dx \tag{13}$$

then

$$a(x_s)\frac{df}{dx_s} + b(x_s)f = -Q_n(x_s) \tag{14}$$

The function $f(x_s)$ that appears in equation (4) can now be determined from the solution of equation (14), together with the initial condition that $f(L) = 0$, where L is the initial liquid level.

Temperature Distribution in Later Period

As mentioned, the later period begins when the exit port first feels the presence of the stratified layer. This occurs when the depth of the stratified layer equals the liquid level. During the later period, the exit port sees a temperature rise due to the temperature profile being carried with the fluid in addition to a temperature rise from heat being added to the system. To account for both of these processes, the assumption is made that

$$\vartheta(x,x_s) = \vartheta_{ref}\left[F(x_s)\Phi(x,x_s) + \Psi(x,x_s)\right] \tag{15}$$

where

$$\Psi(x,x_s) = \left(1.0 - \frac{x_s - x}{x_{s,l}}\right)^n \quad 0 \le x \le x_s \tag{16}$$

$$\Phi(x,x_s) = 1.0 - \left(1.0 - \frac{x_s - x}{x_{s,l}}\right)^n \quad 0 \le x \le x_s \tag{17}$$

Equation (15) satisfies the condition that at $x_s = x_{s,l}$, the temperature profiles are matched provided

$$F(x_{s,l}) = f(x_{s,l})$$

Introducing equation (15) into the energy equation and simplifying

$$\alpha(x_s)\frac{dG}{dx_s} - \beta(x_s)G = Q(x_s) \tag{18}$$

where

$$G(x_s) = 1.0 - F(x_s) \tag{19}$$

$$\alpha(x_s) = \int_0^{x_s} \Phi(x,x_s)A(x)dx \tag{20}$$

$$\beta(x_s) = \int_0^{x_s} \Psi(x,x_s)A(x)dx - \Psi(0,x_s)A(x_s) \tag{21}$$

$$Q(x_s) = Q_w(x_s) + Q_n(x_s) \tag{22}$$

Equation (18) together with the initial condition that $G(x_{s,l}) = 1.0 - f(x_{s,l})$ comprise the mathematical formulation of the problem in the later period.

LIQUID HYDROGEN EXPERIMENTS

In the previous sections, it was shown how data from the infrared radiation program provided the fundamental assumptions for a propellant heating analytical flow model. This analysis will now be applied to the results of two liquid hydrogen experiments. One of the experiments conducted at the Lewis Research Center consists of studies wherein only the walls of the tank are heated. In the other, neutron and gamma ray radiation from a nuclear reactor provided the mechanism for heat generation in the tank walls and internally in the fluid. The latter effort was conducted under contract to the General Dynamics Corporation, Fort Worth, Texas.

Wall Heating Experiments

These experiments were conducted primarily to test the application of the analytical flow model to liquid hydrogen. Tests were conducted in which wall heating was applied to both the side walls and to the bottom wall of the tank. Comparisons are then made between the experimental and the analytical results.

Apparatus and procedure. - The liquid hydrogen wall heating experiments were conducted using a cylindrical tank with a conical bottom having a nominal liquid capacity of 125 gallons (fig. 6). The 32-inch-diameter cylindrical walls joined with a spherical zone to a frustrum of a 45° half-angle cone. The cone was terminated by joining to a 4.8-inch-diameter spherical segment. A 3/4-inch schedule 40 pipe attached to the bottom

provided for the egress of liquid. The test tank was suspended inside an evacuated shell, which provided thermal insulation. Means for introducing gaseous hydrogen at ambient temperature (~60° F) was provided to pressurize and maintain tank pressure with a minimum disturbance to the liquid surface. Liquid outflow was measured using a venturi and was maintained constant by adjustment of a throttle valve. Wall heating was controlled to the cylindrical tank wall and to the tank bottom using electric radiant heaters suspended in the vacuum space. Temperatures at several axial locations were measured using carbon resistors attached to a rake extending down the centerline of the tank.

Results and discussion. - Two tests are presented for which the pertinent test conditions are shown in the following table:

Test	Heat flux, watts/ft^2	Initial height of liquid, ft	Initial temperature, $^\circ$R	Flow rate, lb/sec	Pressure, psia
1	3.32	3.69	38.53	0.0398	34.5
2	9.23	3.61	38.45	.0396	34.5

In the first test the same heat flux was used for both the tank wall and the tank bottom. The second test was essentially a repeat of the first except that the value of heat flux was increased from 3.32 to 9.23 watts per square foot.

The measured temperature history for tests one and two are presented in figures 7(a) and 7(b), respectively. The temperature rise after the start of flow is shown for several heights along the tank centerline. The dotted line normal to each curve indicates the temperature rise necessary to achieve saturation at each height. The dashed lines show the corresponding analytical predictions obtained from the analysis using the test

conditions of the preceding table as input data. For these predictions the heat flux below the cylindrical wall was considered as contributing to bulk heating, whereas the cylindrical wall heat flux contributed to boundary layer flow.

A comparison of the measured temperature rise below the liquid surface shows that only a slight gradient existed in the bulk of liquid for either test. Although this gradient was about the same for each test, the magnitude of the temperature rise of the liquid bulk was proportional to the heat flux. As the liquid surface approaches each sensor, the temperature rises rapidly to the saturation temperature, thus indicating the stratified layer above the bulk of liquid.

A comparison between the measured temperature rise (solid line) and the calculated temperature rise (dashed line) indicates general agreement existing (fig. 7). The calculated temperature profiles, however, did not indicate as large a temperature gradient in the hydrogen as was indicated by experiment. This was due to the use of a simplified expression for the exponent n, equation (10). The discrepancies between the measured and calculated temperature histories at the tank exit (sensor height, 0 in.) was due to slight uncertainties in the measured heating rates.

Nuclear Radiation Experiments

A series of tests were conducted under contract to the General Dynamics Corporation, Fort Worth, Texas, to obtain propellant heating data using a nuclear reactor as the energy source (ref. 6). The experimental effort was composed of three series of tests: nuclear radiation

flux mapping, gross heat determination, and flow characteristics studies. The first two were fundamental to establishing the test environment for interpreting the results of the flow studies.

Apparatus and procedure. - The test configuration employed is shown in figure 8. A test tank, geometrically identical to the one used in the wall heating experiments, was mounted above the Aerospace Systems Test Reactor (ASTR) at General Dynamics Corporation. The tank was insulated to provide a maximum ambient heat leak of 50 watts. The Dewar assembly was surrounded by a liner tank that functioned as a barrier from the shield water. This shielding was necessary to prevent excessive radiation exposure to personnel outside of the immediate area. The arrangement was such that the reactor could be positioned either immediately adjacent to the liner tank or separated from it with water between the two. This water, by virtue of its shielding properties, enabled testing with different heating rate gradients in the liquid hydrogen.

Platinum resistance thermometers were positioned throughout the tank to yield temperature histories in the liquid and ullage gas. Other measurements included radiation level, pressure, and liquid and gas mass flow rates.

Neutron and gamma ray fluxes, which were used to calculate the heat deposition rates, were determined by both experiment and calculation. The calculated values were obtained by use of the C-17 computer code (ref. 7). The measured values were obtained by irradiation of neutron foils and gamma ray dosimeters mounted throughout the system. Irradiations were conducted with and without liquid hydrogen in the tank.

For further verification of the gross heating of the system, self-pressurization tests were also conducted. Temperatures in the liquid and ullage gas and ullage pressure were measured as a function of time when the reactor was at power and the tank closed. An energy balance yielded the gross heating of the system. Tests were repeated for several initial liquid levels.

In addition to nuclear heating, the hydrogen receives heat from the following ambient thermal processes: conduction from instrument leads, other penetrations and the insulation, and thermal radiation from the outer shell. The value of this ambient heat leak was also obtained from self-pressurization tests.

For the final series of tests, hydrogen was permitted to flow from the tank at approximately 0.04 pound per second. (The actual flow rate varied somewhat from run to run and in some cases during the course of the run). During these runs, the ullage pressure was held constant at a value of about 30 psia.

The initial step for the flow runs was to achieve the desired tank pressure. The reactor was then taken to the appropriate power level; immediately thereafter, flow was started. Data were taken prior to and during the flow portion of the test.

Results and discussion. - In general, agreement between measured and calculated radiation flux values was within ±20 percent. (No further discussion will be conducted here regarding the radiation fluxes since a complete summary appears in ref. 6.) The data presented in figure 9 show the manner in which the radiation attenuated through the hydrogen. Since heating rates are directly proportional to reactor power level, the values

presented on the figure have been normalized to a reactor power of 1 megawatt. It is seen here that for both configurations more heat is deposited in the liquid near the bottom of the tank than near the top. This difference is more pronounced for configuration I than for configuration II and is a direct result of the addition of 4 inches of water between the reactor and tank for configuration II. This water serves as a shield against radiation reducing the neutron flux by about a factor of five and the gamma ray flux by a factor of two. Thus by having the 4 inches of water in configuration II, eliminating much of the neutron flux, the heating gradient in the tank assumes a distribution more like that of the gamma rays; having less attenuation through the hydrogen.

The gross heating of system was determined by (a) integrating the calculated nuclear data and by (b) calculations from self-pressurizing data. The shapes of the curves generated by the two methods were very similar although the magnitudes of corresponding values differed by about 20 percent. Most of this difference can be accounted for by the fact that the program used for the nuclear calculations could not accommodate particles with energies less than 0.1 Mev. In view of this it was concluded that the heating obtained from the self-pressurizing tests represented a truer measure of the gross heating and, as such, should be used in analyzing the experimental results.

Figures 10(a) and 10(b) are composite graphs of heating rate showing the contributions of ambient, nuclear wall, and nuclear source heating as functions of liquid level. Figure 10(a) shows data for configuration I and figure 10(b) presents that for configuration II. Inasmuch as the

nuclear and nuclear wall heating are proportional to reactor power, the curves have been normalized to a power of 1 megawatt. The ambient heating curves are independent of power lever. The data points shown on the two figures correspond to the actual self-pressurization data. Total heating curves were generated by adjusting the nuclear derived heating distributions to self-pressurization data at one point. The shaded symbol shows the point of adjustment. The ambient heating curves are identical since they are independent of configuration, but the values of nuclear wall and source heating rates are quite different.

The test parameters for the two flow tests presented are as follows:

Test configuration	Reactor power, megawatt	Initial height of liquid, ft	Initial temperature, ^{o}R	Flow rate, lb/sec	Pressure psia
Configuration I	0.55	3.44	37.0	0.039	30
Configuration II (4 in. of water)	.985	3.60	37.5	.055	29.8

The major difference between the two tests is that of reactor configuration and thus heating distribution in the hydrogen. The reactor power level was adjusted to yield approximately the same final bulk temperature rise. Attempts were made to have the other parameters the same although it can be seen that they differed slightly.

The heating rates for the two tests can be obtained from figures 10(a) and 10(b) by multiplying the nuclear contributions by the proper reactor power level. The wall heating curves for the two tests are very nearly the same and the total source heating is about the same but the shape of the curves differ.

The temperature histories obtained with reactor-tank configurations I and II are presented in figures 11(a) and 11(b), respectively. Data for several sensors located on the vertical axis are presented. The temperature rise at each sensor location, in the time period prior to the liquid surface passing that probe, indicated a uniform bulk temperature rise. As the liquid surface approached the sensor, a rapid rise in temperature was indicated. This was caused by the stratified layer passing that probe. A comparison of the experimental data (symbols) with analysis (dashed line) indicates the same trend. Using the input data presented in the table of this section, the analysis, in general, was able to predict the temperature history at each sensor location with reasonable accuracy. Once again, the assumption was made that all the heat in the section below the cylinder be assigned to bulk heating.

CONCLUDING REMARKS

This paper has described an approximate method to obtain the temperature history of a fluid contained in a tank which is subjected to nuclear and wall heating. Under conditions of relatively low wall heat flux, with and without nuclear heating, the temperature profiles obtained from the analysis agree well with experimental data. However, the temperature gradients in the fluid differ slightly. With higher amounts of wall heating, this difference is more pronounced. This was caused primarily by the use of a simplified expression for the exponent used in describing the temperature profile. The approximate technique of assuming a plausible temperature profile that is made to satisfy conservation of energy gives sufficiently accurate results to warrant further exploration.

Although the gross aspects of the propellant heating problem have been determined herein, the important question of the detailed fluid description under actual flight conditions where many more factors are introduced is yet to be determined.

REFERENCES

1. Chin, J. H.: Dimensionless Analysis for Non-Draining Cylindrical Propellant Tank. Internal Memo. TSN/10, Lockheed Missiles and Space Co., Sept. 1962.

2. Tatom, J. W., Knight, L. H., Brown, W. B., and Grady, T. A.: Free Convection in Rocket Propellant Tanks. Rep. ER-6216, Lockheed Nuclear Products, Lockheed-Georgia Co., May 1963.

3. Vliet, G.: Stratified Layer Flow Model, A Numerical Approach to Temperature Stratification in Liquids Contained in Heated Vessels. Rep. NSP-64-02, Lockheed Missiles and Space Co., Apr. 1964.

4. Anderson, B. H., and Kolar, M. J.: Experimental Investigation of the Behavior of a Confined Fluid Subjected to Nonuniform Source and Wall Heating. NASA TN D-2079, 1963.

5. Eckert, E. R., and Drake, R. M.: Heat and Mass Transfer. Second ed., McGraw-Hill Book Co., Inc., 1959

6. Hehs, W. A., Cauley, B. M., Miller, G. E., and Wheeler, D. M.: Nuclear Radiation Heating in Liquid Hydrogen. NASA CR-54078, 1964.

7. Hehs, W. A., and Miller, G. E.: Measured and Calculated Nuclear Radiation Distributions in Liquid Hydrogen. NASA CR-54003, 1964.

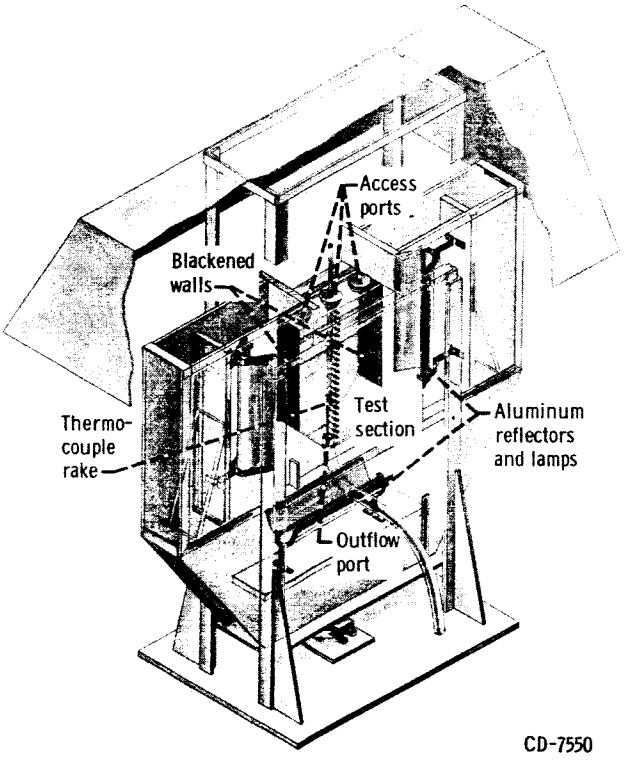

Figure 1. - Schematic diagram of test apparatus.

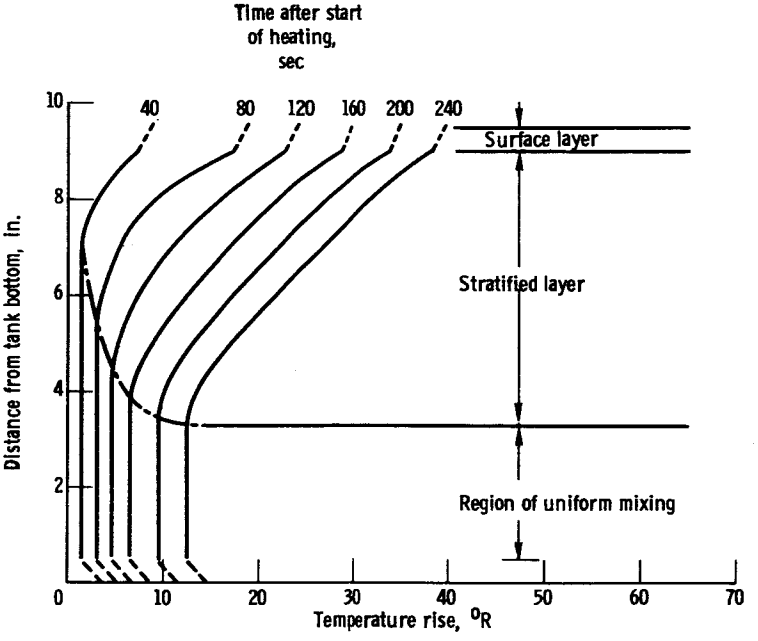

Figure 2. - Axial temperature distribution with wall and nonuniform-source heating, nonflowing system.

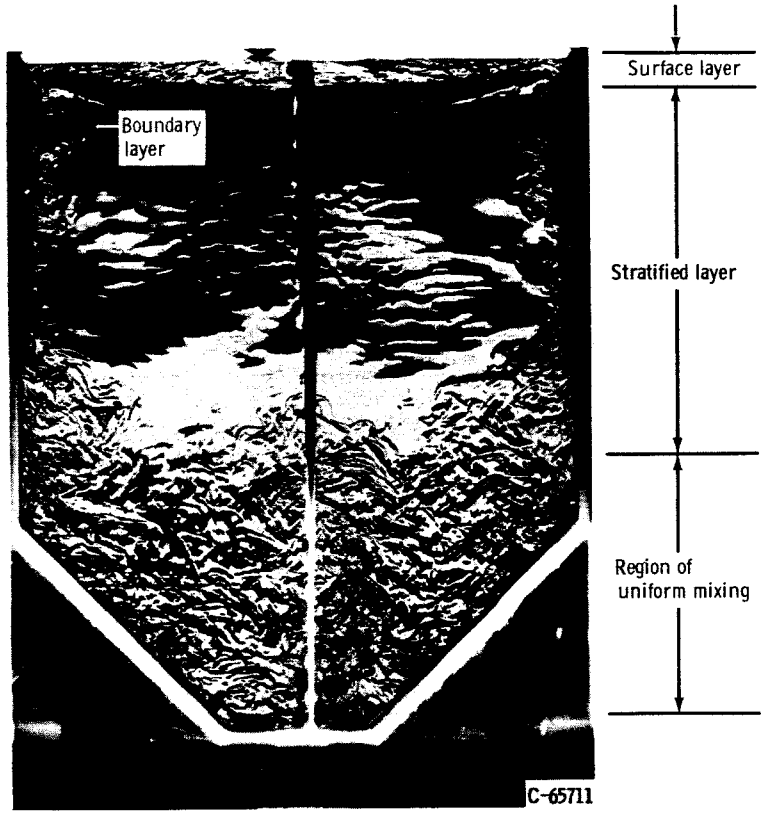

Figure 3. - Schlieren photographs showing flow patterns resulting from nonuniform source and wall heating.

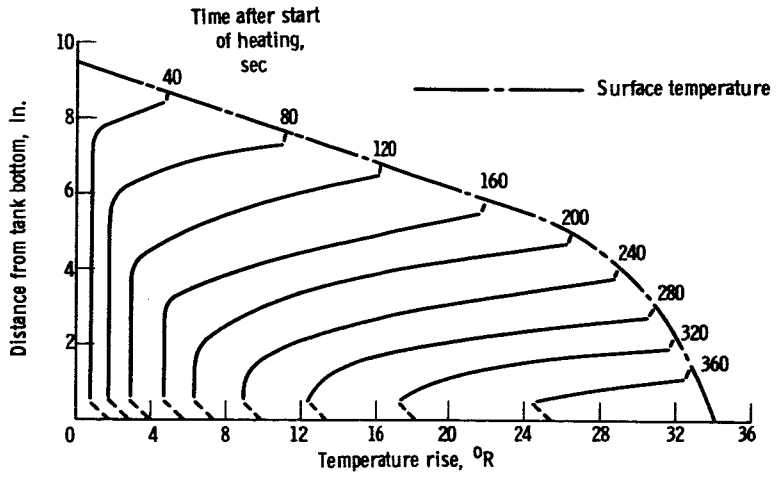

Figure 4. - Axial temperature distribution with wall and nonuniform-source heating, flowing system.

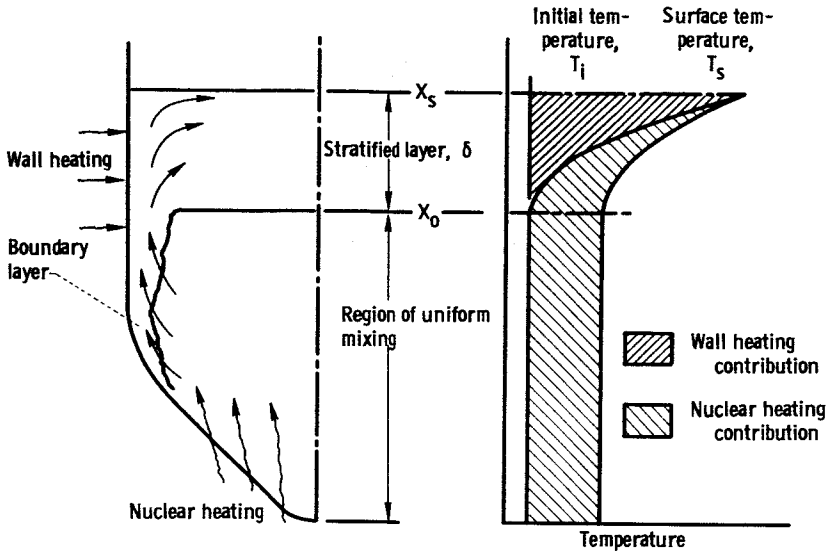

Figure 5. - Schematic diagram of flow model.

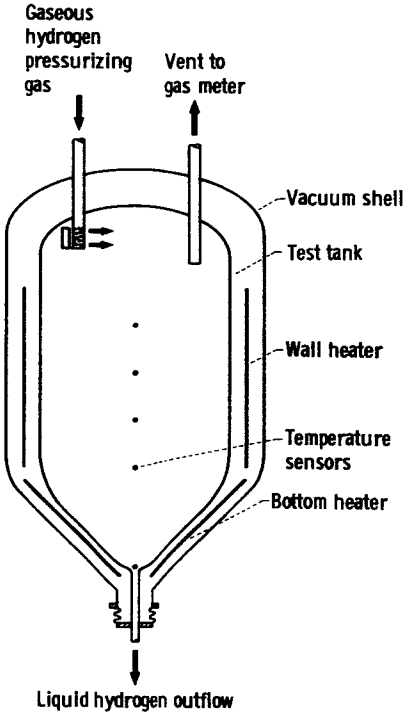

Figure 6. - Electric tank heating experiment.

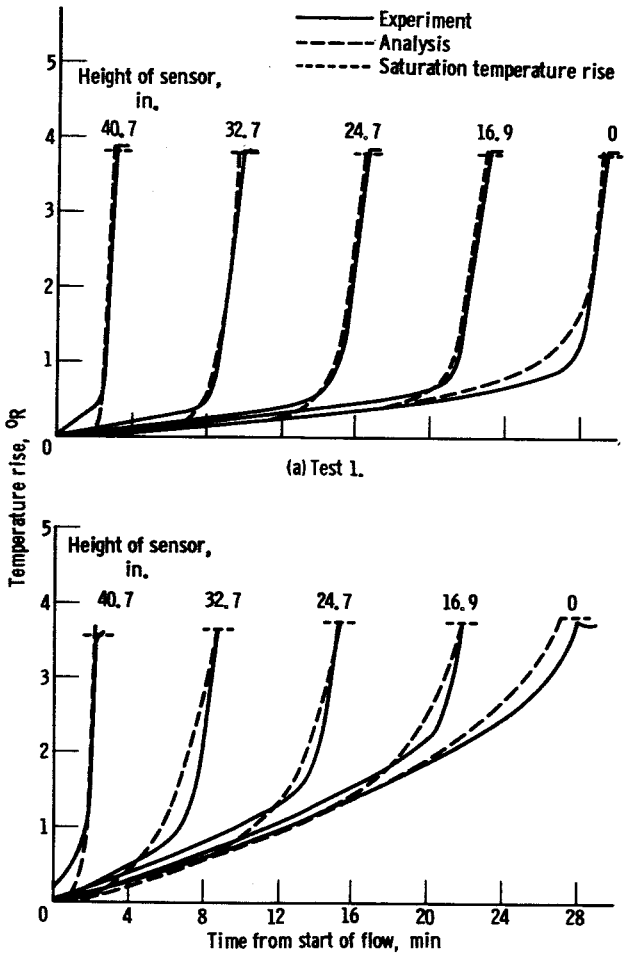

(a) Test 1.

(b) Test 2.

Figure 7. - Temperature history of liquid hydrogen wall-heating experiment.

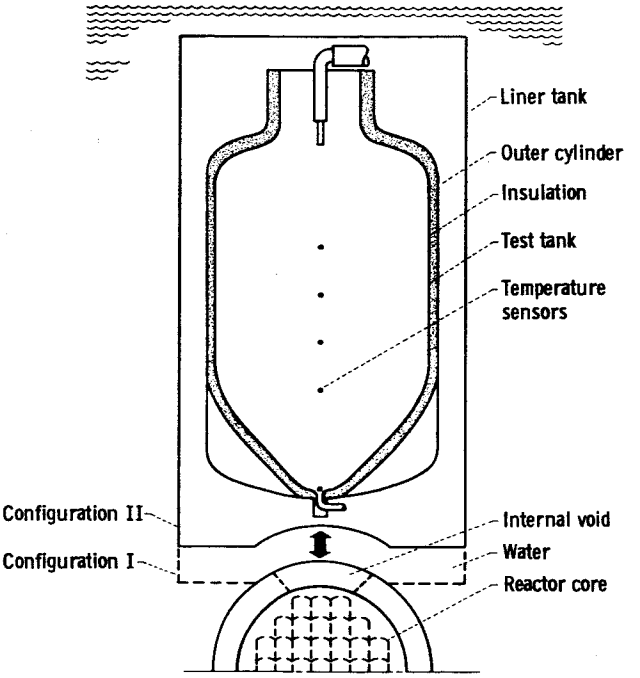

Figure 8. - Nuclear tank heating experiment.

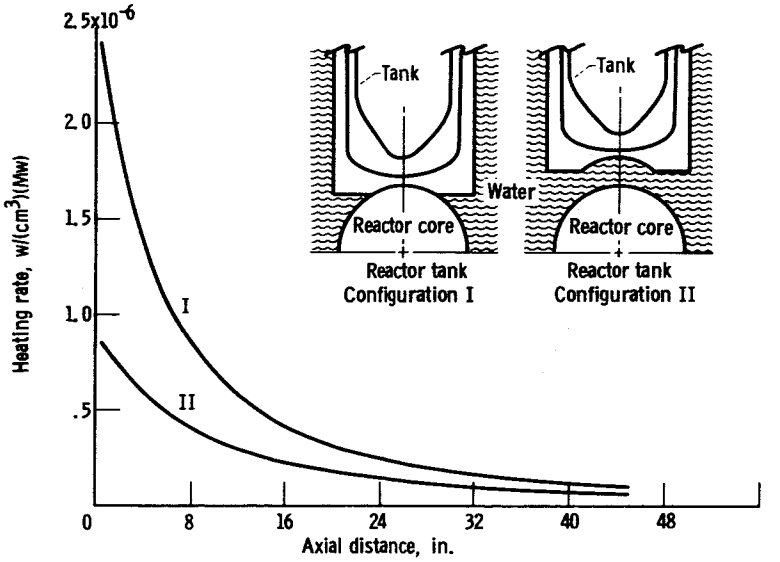

Figure 9. - Test tank centerline heating rates in liquid hydrogen per megawatt of reactor power.

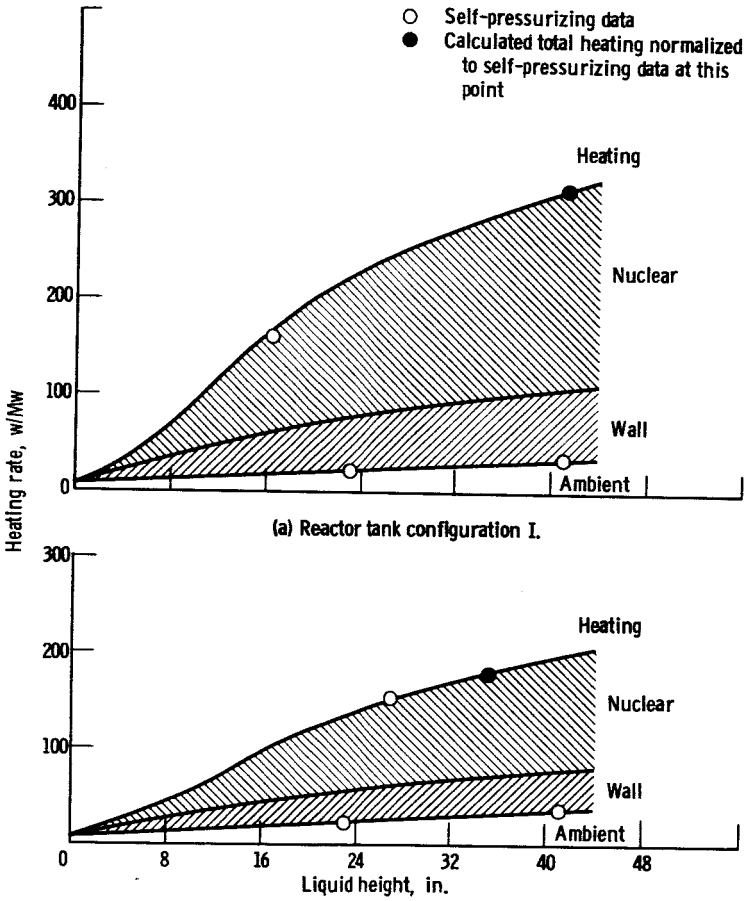

(a) Reactor tank configuration I.

(b) Reactor tank configuration II.

Figure 10. - Total heating in liquid hydrogen per megawatt of reactor power.

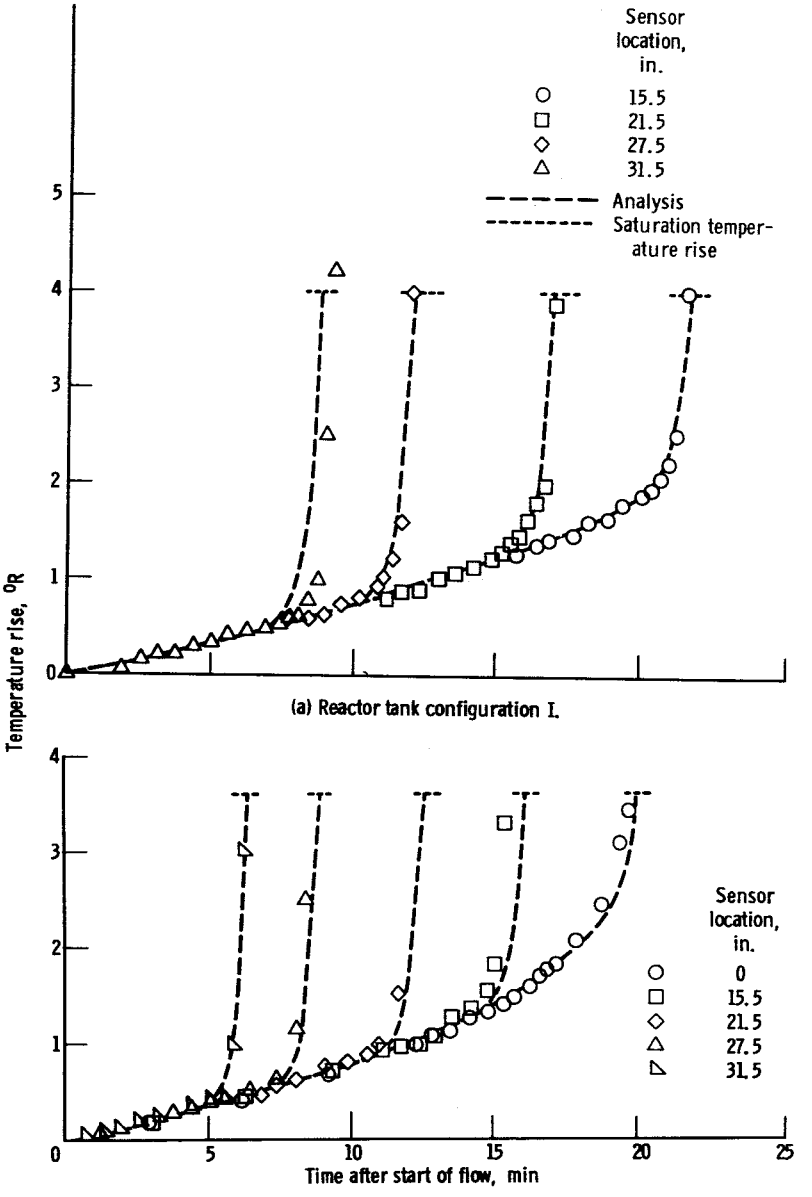

Figure 11. - Temperature history of liquid hydrogen nuclear heating experiment.